Microscopic Features of Methacrylate Polymers with Zwitterionic Pendant Groups Determined by Various Techniques

J. CARDOSO, RAÚL MONTIEL, ALFONSO HUANOSTA-TERA*

UAM-I, CBI, Departamento de Física, Apartado. Postal 55-534, Codigo Postal 09340 México, Distrito Federal, México

Received 11 October 2004; revised 17 December 2004; accepted 21 December 2004
DOI: 10.1002/polb.20404
Published online in Wiley InterScience (www.interscience.wiley.com).

ABSTRACT: The objective of this work was to determine microscopic structural features of three methacrylate polymers with different numbers of diethylene glycol residues and zwitterionic pendant groups. X-ray diffraction, electron microscopy, and scanning probe microscopy techniques were employed. X-ray data led to the adoption of a model made up of molecular aggregates forming lamellar domains, establishing in this way ordered characteristics of these kinds of polymers. Scanning electron microscopy images provided evidence of the occurrence of a lamellar structure forming the morphology of the polymers. This was corroborated by atomic force microscopy experiments. Transmission electron microscopy revealed that the lamellar aggregates conformed into clusters immersed in a polymeric matrix. From phase-contrast images, information on the homogeneity of the composition at a molecular surface level was obtained. Then, the techniques provided evidence of the lamellar domain characteristics of the studied sulfobetaines. The crystallinity was a function of the number of ethoxy groups because as this number increased, the crystallinity became lower © 2005 Wiley Periodicals, Inc. J Polym Sci Part B: Polym Phys 43: 1152–1160, 2005
Keywords: morphology; transmission electron microscopy; atomic force microscopy

INTRODUCTION

Methacrylate polymers with zwitterionic pendant groups have attracted great attention[1–3] because of their very interesting properties in the solid state, such as ionic conduction.[4,5] Zwitterionic polymers have shown specific and unique properties, such as antipolyelectrolyte behavior, strong binding capacity, and high solvation power of glassy polymeric matrices toward salts of different lattice energies. All these interesting properties are due to the high dipole moment in these kinds of polymers. Some possible applications are flocculants and solid electrolytes for high-energy batteries.

According to previous studies,[5,6] zwitterionic polymers show the presence of ionic aggregates in the solid state. The morphology of the polymers is related to their ionic content, showing clusters larger than those observed in ionomers. Castaño et al.[6] argued that these aggregates are densely packed and that this packing depends on the zwitterionic content of the sample and on the length of the lateral chain. Montiel and Manzur[7] proposed a model for zwitterionic clustering that assumes the presence of core–shell structures, with a core of ion pairs surrounded by a shell of hydrocarbon chains 32 nm in diameter. This value is higher than the diameter of the core–shell ionomer structure (ca. 7 nm) because of the loosely packed grain structure.

On the other hand, the methacrylate polymers with zwitterionic pendant groups reported in this article have shown interesting characteristics: a high concentration of polar

*On sabbatical leave from Instituto de Investigacion en Materials-Universidad Nacional Autonoma de Mexico (IIM-UNAM).
Correspondence to: J. Cardoso (E-mail: jcam@xanum.uam.mx)

Journal of Polymer Science: Part B: Polymer Physics, Vol. 43, 1152–1160 (2005)

groups that might contribute to fast ionic transport and a low glass-transition temperature due to the high flexibility of the lateral chain.[4] Variations in the backbone structure result in a variety of different physical properties. For example, increasing the ethylene glycol residues affects physical properties, such as the conductivity and glass-transition temperature, associated with some ordered phases in the polymers that avoid higher conductivity at low temperatures.

In this article, we propose a structural model supported by experimental data from the X-ray scattering of three methacrylate polymers with a system of zwitterionic pendant groups. This research was aimed at providing additional evidence on the microstructure (crystallinity) and macrostructure (morphology) in the ordered phases of these polymer systems. Wide-angle X-ray scattering (WAXS) and small-angle X-ray scattering (SAXS) were used to obtain information on the spatial arrangement at various length scales. Models of the microstructure and morphology are proposed for the samples. The SAXS experimental data were processed with a general computing program presented by Vonk,[8,9] Ruland,[10] and Hosemann.[11] The absolute intensity was calculated according to the method reported by Kratky et al.[12] The data were corrected for finite slit dimensions, background radiation, and absorption calibration.

This study was also devoted to determining the microtopographic characteristics of the aforementioned zwitterionic methacrylates of the sulfobetaine type. Studies were carried out with scanning probe microscopy (SPM), transmission electron microscopy (TEM), and scanning electron microscopy (SEM). A plausible microscopic structural model was built on the basis of these techniques.

Because an up-to-date variant of SPM or atomic force microscopy (AFM) methods has been developed, this technique was particularly applied in a dynamic mode, the so-called tapping or intermittent contact mode. To verify the proposed model, we combined AFM results with TEM and SEM observations.

EXPERIMENTAL

The preparation of methacrylate polymers with zwitterionic pendant groups has been described elsewhere.[4] Three zwitterionic methacrylates of the sulfobetaine type were synthesized through the reaction of 2-(2-N, N-diethylamine-ethoxy)-ethylmethacrylate and 2-(2-(2-N, N-diethylamine-ethoxy)-ethoxy)ethylmethacrylate with butanosultone for the preparation of monomers with various flexibilities. The resulting polymers were characterized by Fourier transform infrared, elemental analysis, and NMR techniques to confirm their chemical structures. Their glass temperatures were determined on a TA 910 differential scanning calorimeter linked to a Thermal Analyzer 2100 microprocessor at a heating rate of 10 °C/min under a 50 mL/min nitrogen flux.

The film samples used in the SAXS and WAXS studies were prepared through the dissolution of the polymers in trifluoroethanol at a concentration of 10%. The solutions were poured into Teflon molds to allow the slow evaporation of the solvent. Then, the films were dried in a vacuum oven at 50 °C for 24 h. The free-solvent film was mounted on a Kratky camera *in vacuo*.

WAXS diffraction patterns of the samples were determined with a horizontal goniometer and an X-ray tube equipped with a copper target, which was powered by a Philips PW1140/60 high-stability generator. Monochromatization was achieved by Bragg's diffraction from a graphite crystal; a Cu Kα target X-ray tube was operated at 40 kV and 50 mA. A proportional counter combined with pulse-height discrimination was used to obtain the SAXS data.

In the other experiments described here, the studies were carried out with pristine polymers; that is, as the materials were synthesized, they had a grainy structure because of their low solubility in the tested solvents. SEM images were obtained with a Cambridge Leica Stereoscan 440. TEM images were collected with a JEOL JEM-EX1200 instrument operated at 120 and 100 keV. TEM studies were performed on finely powdered samples obtained by the grinding of the pristine materials. The powdered products were deposited by gravity on support film grids. As for the AFM observations, all SPM imaging experiments were performed in air at room temperature. A JSPM-4210 scanning probe microscope was used to carry out the AFM observations. AFM experiments were generally carried out with silicon cantilevers, which had tips with a curvature radius of less than 10 nm (SC12 series ultrasharp cantilevers, MikroMash), a tip height of 15–20 μm, and a full tip angle of less than 20°. Other cantilever features are mentioned as necessary.

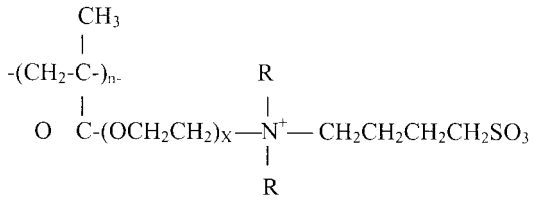

Sample	X	R
PMBS-1	1	$-CH_3$
PMBS-2	2	$-CH_2-CH_3$
PMBS-3	3	$-CH_2-CH_3$

Figure 1. Schematic structure of the studied polymers.

RESULTS AND DISCUSSION

Figure 1 shows the general structure of the flexible polymethacrylates in which monomeric dialkylamine monoethylene glycol, diethylene glycol, and triethylene glycol sulfobetaines were synthesized. X represents a diethylene glycol residue. Spectroscopic characterization ensured the identity of the chemical structure.

The glass-transition and decomposition temperatures were determined for the three polymers. They were 261 and 295 °C, 95 and 281 °C, and 27 and 296 °C for polymethacrylate butane sultone (PMBS)-1, PMBS-2, and PMBS-3, respectively; the numbers 1, 2, and 3 are the numbers of OCH_2CH_2 units. The glass-transition temperature decreased as the flexibility of the lateral chain increased, and this depended on the X value. The decomposition temperature of the synthesized polymers was almost constant. These temperatures were not significantly dependent on X.

Figure 2 shows WAXS data for the PMBS1, PMBS2, and PMBS3 samples. Although a well-developed crystalline system could not be

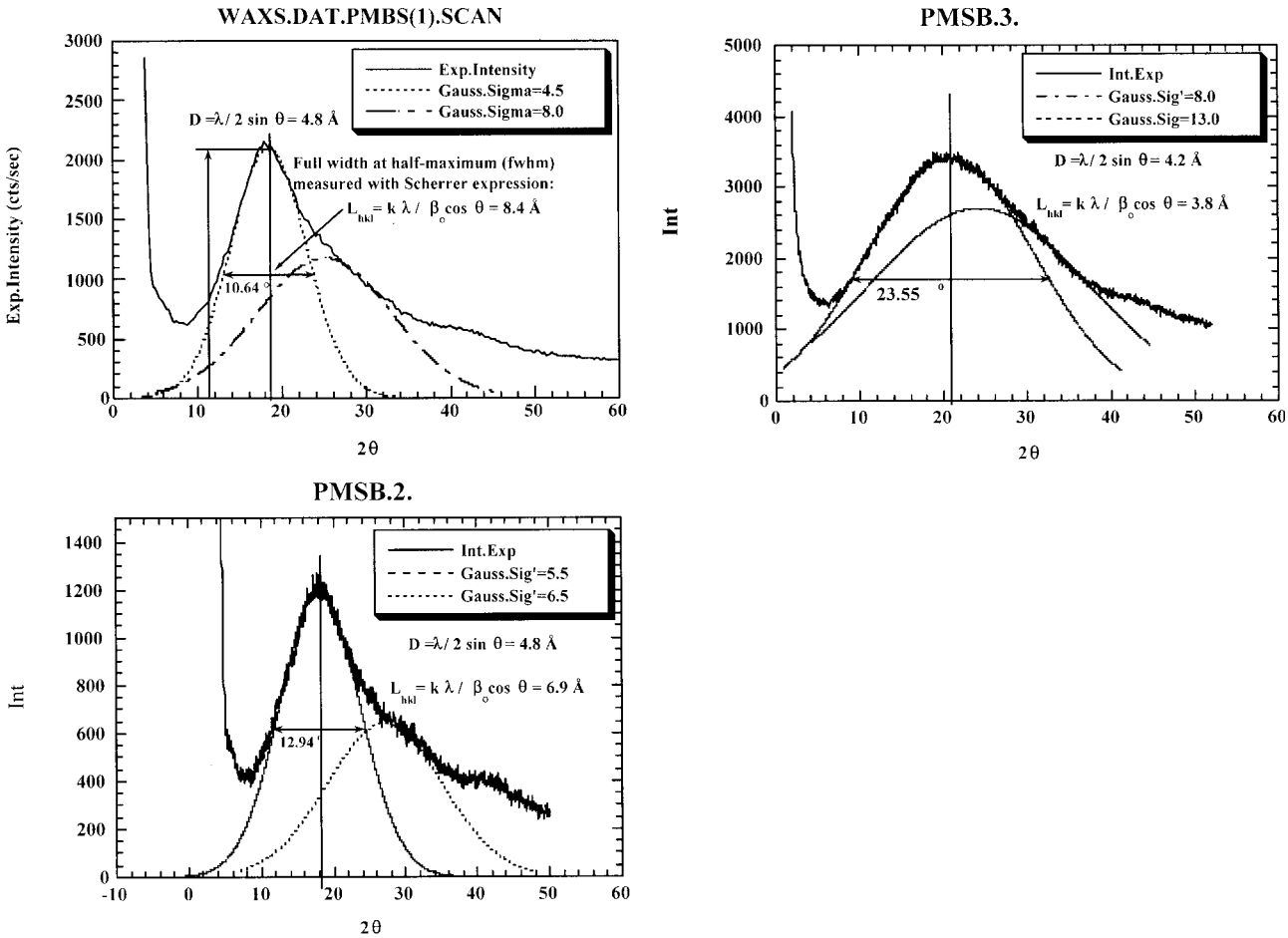

Figure 2. WAXS data for PMBS-1, PMBS-2, and PMBS-3 (methacrylate polymers with zwitterionic pendant groups; D = interplanar spacing, from Bragg law, Exp = experimental, Int = intensity, Sig = sigma = σ, Gauss = Gaussian curve).

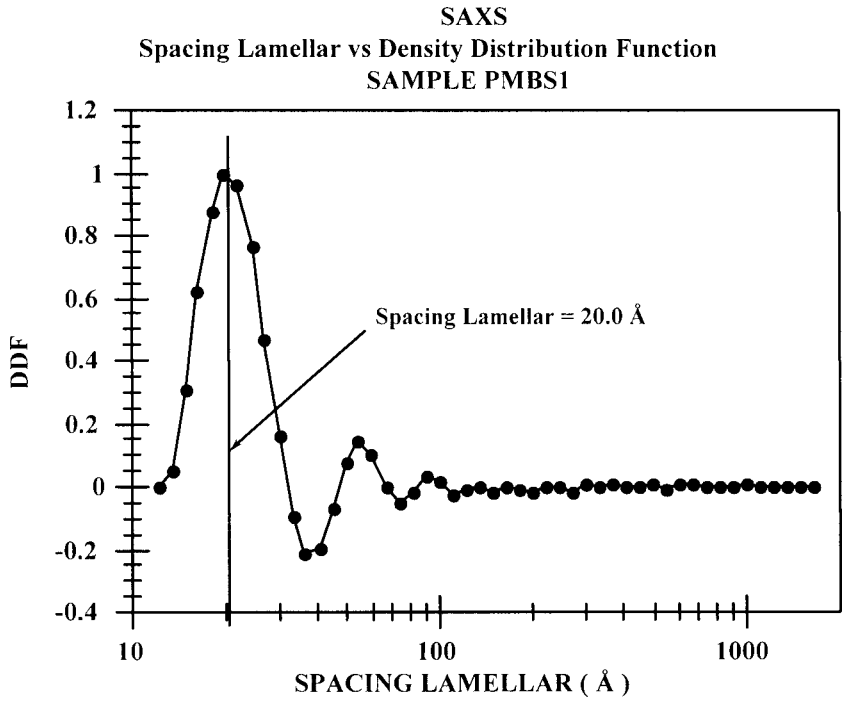

Figure 3. Distribution function (DDF) versus the lamellar spacing.

observed in the WAXS diffraction pattern, the broad diffraction peak at a scattering angle close to 20° indicated the presence of some ordered structure.

An alternative quantification of this structure was the measurement of the mean size of the crystalline domain with the Scherrer equation: $L_{hkl} = K\lambda/\beta_0 \cos\theta$. L_{hkl} describes the mean crystal dimension normal to the *hkl* plane, β_0 is the half-height width of the scattering peak at 2θ, λ is the radiating wavelength, and K is a constant ($\cong 1$). For PMBS1 with $K = 1$, $\lambda = 1.54$ Å, $\beta_0 = 10.64°$, and $2\theta = 18.5°$, we obtained $L_{hkl} = 8.4$ Å.

The processed data from the SAXS experiments, shown in Figure 3, which correspond to the density distribution function plotted against the lamellar spacing of the domains, together with the aforementioned WAXS results, support the morphology proposed in the pictorial representation shown in Figure 4, which can be considered an ordered arrangement of lamellar aggregates.

This conclusion was reached after the theoretically generated data were fitted to the experimental SAXS data for several test functions related to different geometrical shapes included in the computer program used.[8,9] In general, the values of the minimum standard deviation of the chosen geometrical shape of the aggregates supplied criteria for the best choice in each case. For PMBS-1, the minimum standard deviation was 5.2, which strongly suggested aggregates with a lamellar form, with L_{hkl} slightly above 8 Å and lamellae interspaced around 20 Å. This is the best model proposed for this case.

WAXS data for the other samples, PMBS-2 and PMBS-3, exhibited slightly broader peaks, which were indicative of poor ordering in the

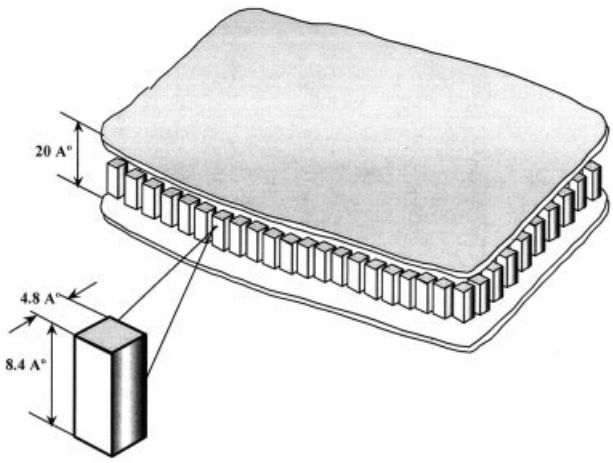

Figure 4. Proposed model describing the arrangement and dimensions of the aggregate of the crystalline cluster and shell.

samples. As a result, even with the best resolution, the Kratky camera did not provide scattering intensity well enough to make a highly reliable determination. In these last cases, the analysis yielded minimum standard deviation values greater than 5, which could not be considered very appropriate values for a properly performed SAXS determination. However, the values for the other parameters were calculated to provide an approximate idea of the form and size of the aggregates. We concluded that although there were also lamellar arrangements forming the PMBS-2 and PMBS-3 polymers, they seemed to be poorly ordered, and the lamellar domains were smaller than those in PMBS1; the microscopy observations of the grainy samples corroborated this conclusion. The corresponding SEM images are shown in Figure 5; the lamellar features of PMBS-1 can be more clearly observed than those of the other polymers.

The specimen surfaces were observed as the polymers were being prepared, the images being acquired from grainy samples. Because the pristine specimens were particularly difficult to hold onto a flat surface, they were fixed onto a piece of double-sided copper tape. The AFM micrographs of the polymer grains revealed both the vertical size and the polymer surface morphology features. The image contrast represents the difference in the tip–surface interactions at different surface sites and shows the existence of nanoscopic-like engraved lamellae in the polymers. The roughness of the surface in the three-dimensional image resembles grooves on a field. The AFM images seemed to show the existence of nanometer platelets (like seeds) packed to form the lamellar structure observed in the SEM images. For PMBS-1, the profile of the three-dimensional topographical image in Figure 6 is shown in Figure 7. The profile plane lies on a plane perpendicular to the grooves.

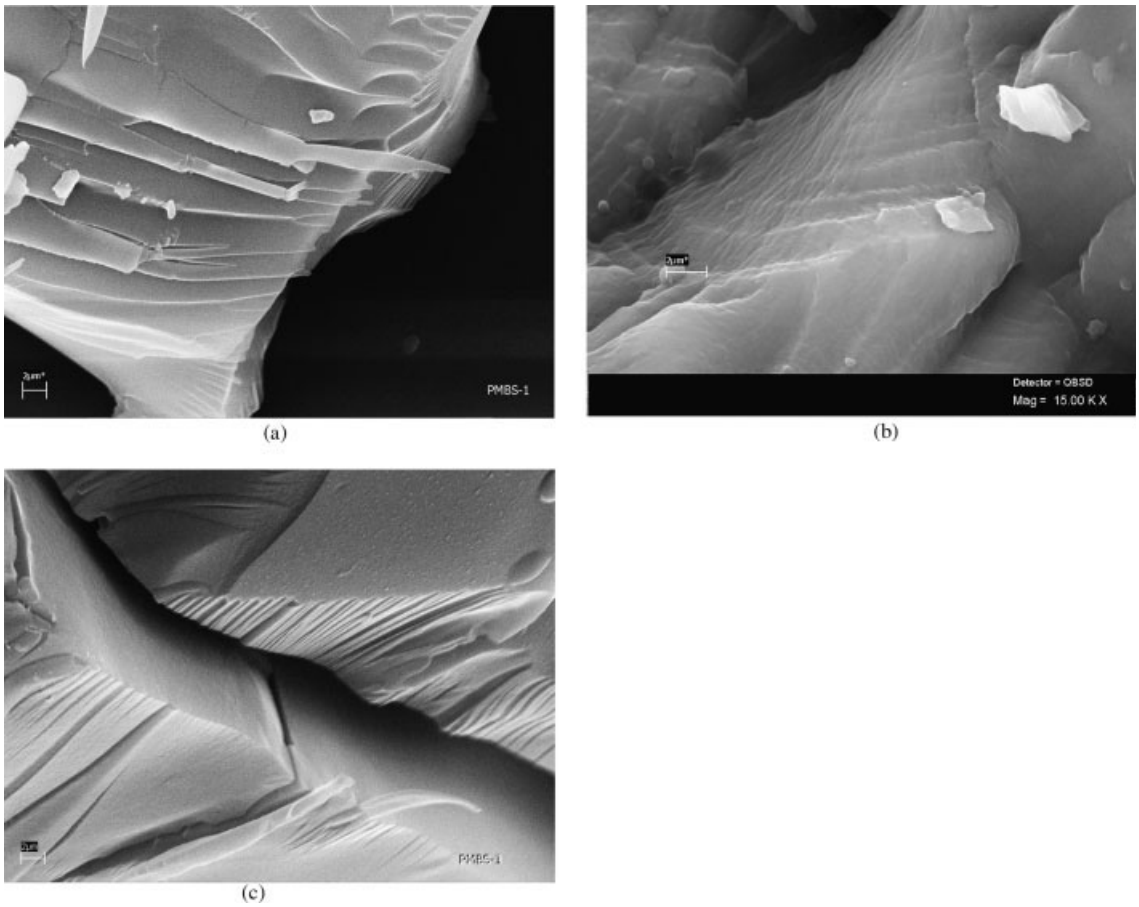

Figure 5. SEM images of (a) PMBS-1,(b) PMBS-2, and (c) PMBS-3. Note the lamellar features of the materials, particularly those of PMBS-1.

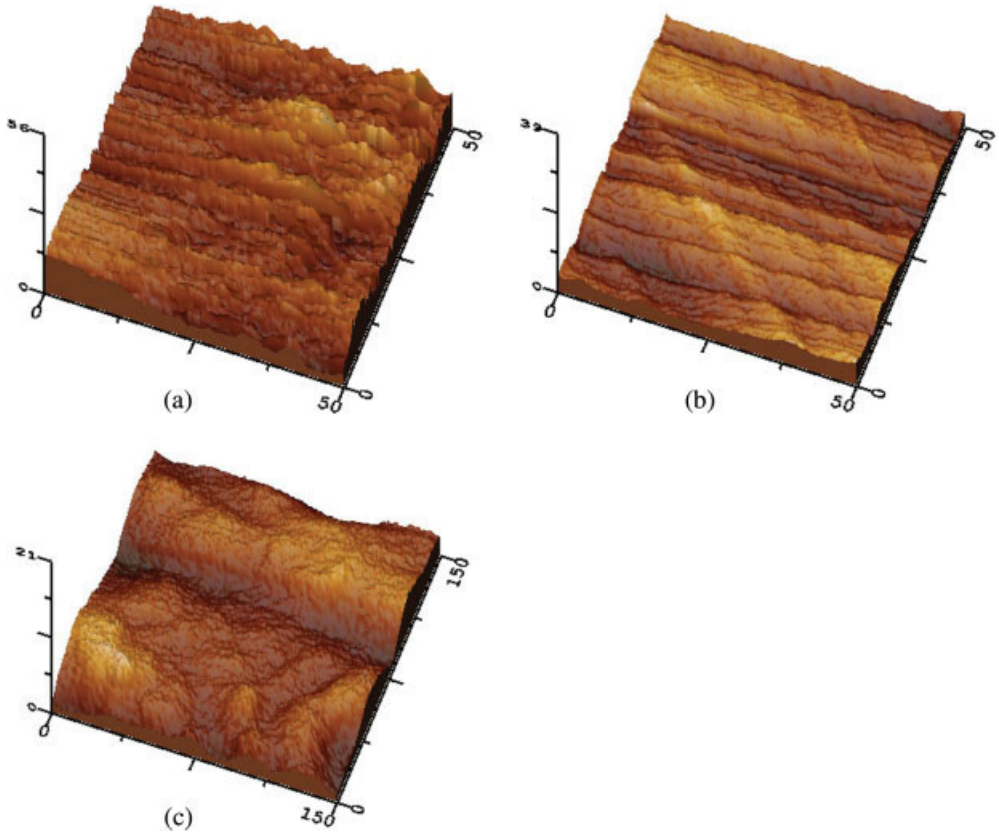

Figure 6. High-resolution AFM images of pristine samples (a) PMBS-1, (b) PMBS-2, and (c) PMBS-3.

The distance of the closest peaks (~0.5 nm) corresponds to the distance of the platelets forming the larger lamellae. We believe that the lamellar aggregates originated from the correlated ionic interactions between zwitterionic chains, the origin of which may be explained as follows. The global neutrality in the polymer was altered locally in the vicinity of the molecular chains by the difference in the polarities between the ionic and hydrophobic parts in the chain itself; the result was a polar entity that could interact electrostatically with the neighboring chains. By this mechanism, large aggregates could be formed.

By mapping the phase lag of the cantilever oscillation during the tapping-mode scan, we obtained phase images of the same regions shown in Figure 5 (Fig. 8). When an AFM tip interacts with a viscoelastic surface, a viscous damping force arises; it depends on the contact size and the penetration of the tip into the material. In fact, in tapping-mode phase imaging, the phase shift depends nonlinearly on the material properties;[13] this technique can differentiate between areas with different properties, regardless of their topographical nature.[14] Furthermore, that phase images may be inter-

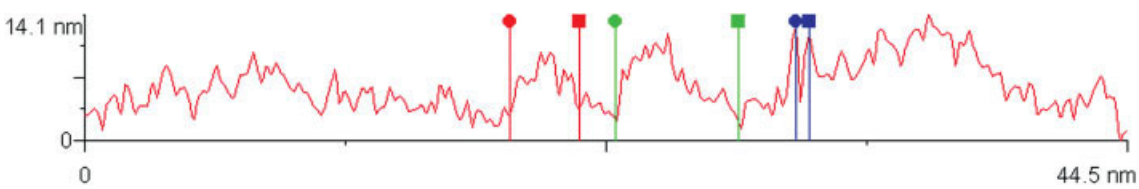

Figure 7. Profile features of the topography of PMBS-1 shown in Figure 5(a). The plane plot lies on a plane perpendicular to the grooves shown in Figure 5(a).

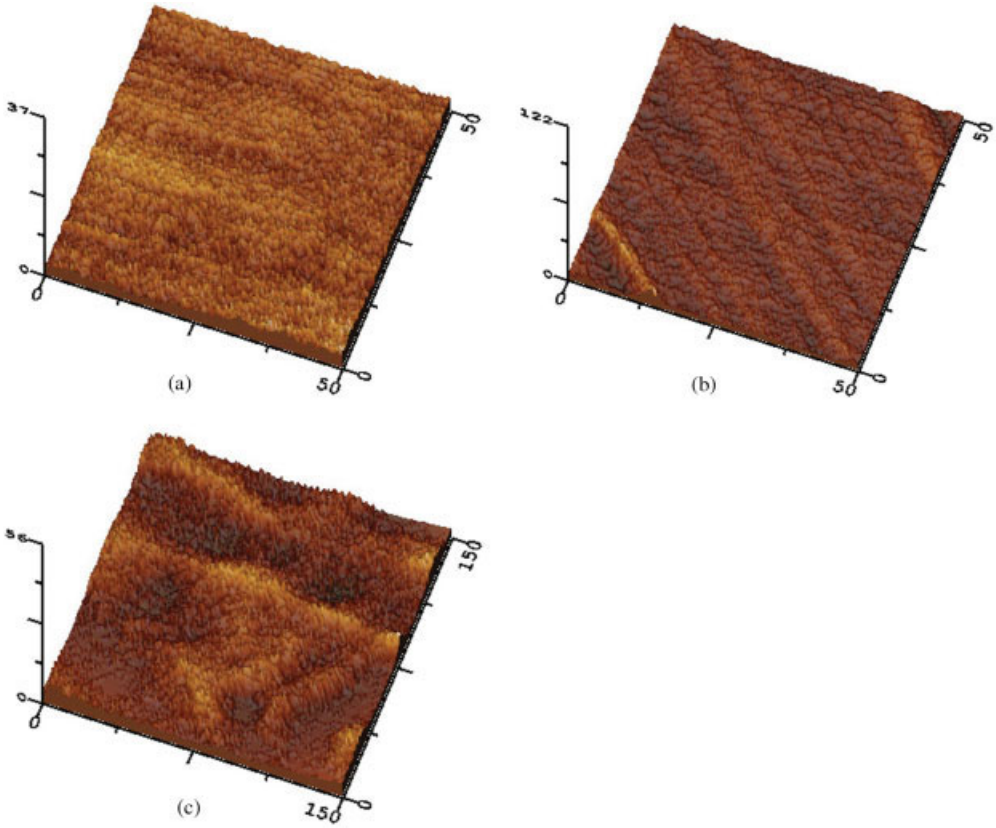

Figure 8. Phase images corresponding to those in Figure 5: (a) PMBS-1, (b) PMBS-2, and (c) PMBS-3.

preted as energy dissipation images for a constant-oscillation amplitude.[15]

The shift of the cantilever phase mapped from the imaged regions in Figure 6 reveals fairly homogeneous surfaces for PMBS-1, PMBS-2, and PMBS-3; that is, the studied methacrylate polymers exhibited unique physical features at this level. Because phase contrast should not depend on topography, the presence of the contrast edge delineating the direction, followed by the grooves in the height images (Fig. 6), made possible the close correlation between the topography and the phase-contrast image. The correspondence between the two images was related to an increase in the effective contact area of the tip cone and to a consequent increase in the energy dissipation; this led to the change in the phase contrast in the edge region.[16]

In the described AFM experiments, cantilevers with a length of 300 μm, a width of 35 μm, a thickness of 2 μm, a resonant frequency of 28 kHz, and a force constant of 0.35 N/m were used.

The selection of a polymeric material for special applications depends not only on the surface microstructure but also on the bulk characteristics. TEM images were recorded for the latter. The TEM images provided direct evidence of the existence of relatively large precipitates embedded in the polymer that scattered the electronic beam more forcefully than the other parts of the material[6] (Fig. 9).

The precipitates, approximately 50 nm in size, had to have been built by the aforementioned laminar aggregates. As explained previously, the laminar entities consisted of aggregated polymeric chains, which remained together because of correlated ionic interactions. The precipitates formed as if they were phase-segregation regions in the polymer. This apparent phase segregation seemed to originate mainly from the ionic interactions occurring between the zwitterionic chains, which were naturally due to the polar character of the molecular chains acquired from the difference in the polarities of the ionic and hydrophobic parts of

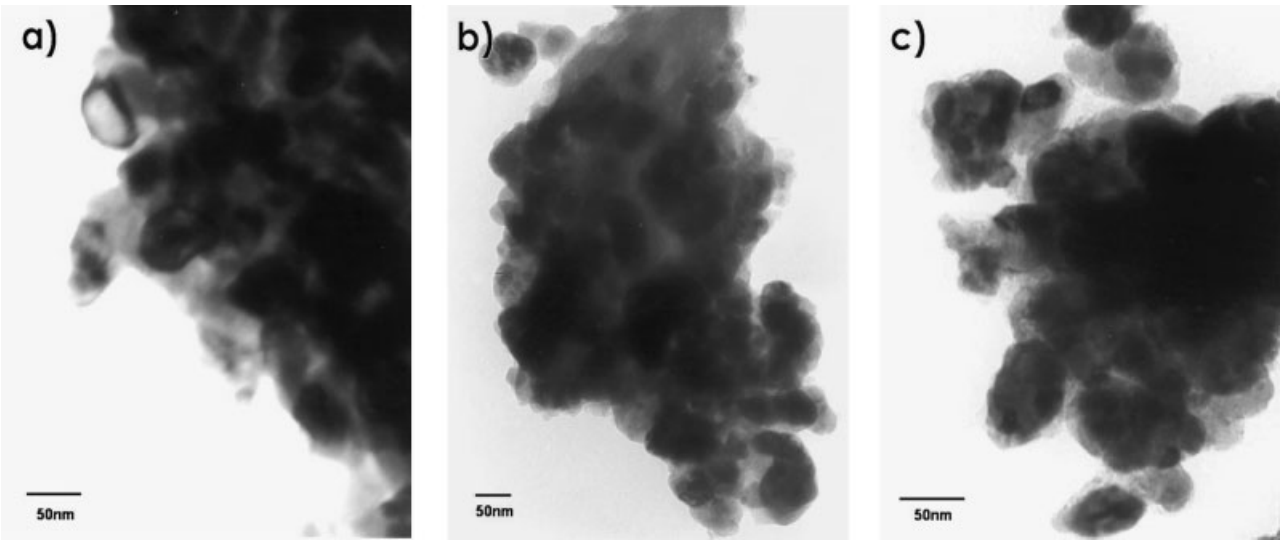

Figure 9. TEM images of the three methacrylate polymers with zwitterionic pendant groups: (a) PMBS-1, (b) PMBS-2, and (c) PMBS-3. The contrast is similar to that of precipitates embedded in a polymeric matrix.

the chains themselves; that is, the precipitates were ion-enriched regions in the polymer and consisted of lamellar domains, which in turn were chain cumuli. Finally, the spatial distribution of the precipitates originated from the observed X-ray dispersion and served to classify as crystalline the studied materials. The ionic interaction determined not only the size and shape of the clusters of the aggregated chains but also the extension of the regions in the polymer in which the absence of ion-enriched groups of chains occurred. In fact, these last regions served as a matrix in which the observed clusters were embedded. This also explained the topography of the AFM images in Figure 5; the peaks in the profile curve are associated with well-constituted lamellar aggregates, whereas the depletions correspond to the material in the matrix. A slight contrast can be appreciated in the small clusters of the TEM images for all the samples (Fig. 5). Because the main constituent atoms of the polymers had quite similar atomic weights, the contrast could not be attributed to the presence of differences in the concentrations of some of the atoms present. Hence, we concluded that the contrast should be associated with the way in which the molecular chains were packed (i.e., the core–shell structure). When we observed samples by TEM, some precautions were taken. To avoid possible damage or changes in the polymers introduced by the interaction between the electron beam and the samples, the current density of the lenses was kept low, and the time spent in taking the micrographs was reduced as much as possible. Furthermore, no staining agent was used to image the polymers.

CONCLUSIONS

The basic morphology of methacrylate polymers with zwitterionic pendant groups was found to be a core–shell configuration of molecular aggregates embedded in an amorphous polymer matrix. Evidence supporting this statement has been presented; we first discussed X-ray data, which led to the adoption of a model made up of molecular aggregates forming lamellar domains. The lamellar features were impressively imaged by SEM and AFM techniques. Interestingly enough, the TEM images showed a contrast very similar to that corresponding to precipitates immersed in a polymeric matrix. This contrast corresponded to a cumulus of lamellar domains, which in turn were formed by agglomerated molecular chains, which finally constituted the precipitates. The spatial distribution of these precipitates determined the X-ray scattering, the characteristics of which supported the already proposed model. In conclusion, the studied sulfobetaines are crystalline systems that can be adequately described by a lamellar structure. As the number of pendant groups increases, the crystallinity decreases, and the lamellar aggregates become smaller. Phase-contrast microscopy was used to obtain information on the composition at the molecular surface

level because the strain response lagged behind the stress by a phase angle, which was characteristic of each material. The observed contrast in the phase images was associated with the difference in the phase lag between neighboring engraved grooves. Taken as if they were a map of the stiffness of the surface features, the phase images did not reveal differences in the viscoelastic energy dissipation properties of the polymers, the sample compositions being uniform.

The authors are indebted to Carlos Flores, J. Guzman-Mendoza, and Jaime Santoyo for technical help.

REFERENCES AND NOTES

1. Monroy-Soto, V. M.; Galin, J. C. Polymer 1984, 25, 121.
2. Galin, M.; Monroy-Soto, V. M.; Galin, J. C. Polymer 1984, 25, 254.
3. Cardoso, J.; Manero, O. J Polym Sci Part B: Polym Phys 1991, 29, 639.
4. Cardoso, J.; Manrique, R.; Albores-Velasco, M.; Huanosta, A. J Polym Sci Part B: Polym Phys 1997, 35, 479.
5. Montiel, R.; Cardoso, J.; Manero, O. J Mater Res 1995, 10, 2106.
6. Castaño, V. M.; González, A. E.; Cardoso, J.; Manero, O.; Monroy, V. M. J Mater Res 1990, 5, 654.
7. Montiel, R.; Manzur, A. J Macromol Sci Phys 1992, 31, 365.
8. Vonk, C. G. J Appl Crystallogr 1975, 8, 340.
9. Vonk, C. G. J Appl Crystallogr 1975, 9, 433.
10. Ruland, W. J Appl Crystallogr 1971, 4, 70.
11. Hosemann, R. J Polym Sci Part C: Polym Symp 1967, 20, 11.
12. Kratky, O.; Piltz, I.; Schmitz, P. J. J Colloid Interface Sci 1966, 21, 24.
13. Scott, W. W.; Bhushan, B. Ultramicroscopy 2003, 97, 151–169.
14. Winkler, R. G.; Spatz, J. P.; Sheiko, S.; Moller, M.; Reineker, P.; Marti, O. Phys Rev B 1996, 54, 8908.
15. James, P. J.; Antognozzi, M.; Tamayo, J.; McMaster, T. J.; Newton, J. M.; Miles, M. J. Langmuir 2001, 17, 349.
16. Magonov, S. In Visualization of Polymer Structure with Atomic Force Microscopy: Applied Scanning Probe Methods; Brushan, B.; Fuchs, H.; Hosaka, S., Eds.; NanoScience and Technology Series; Springer: Berlin, 2004; pp 207–251.